

Breathing response in a statically indeterminate cracked rotor

Declan Williams and Helen Wu

School of Computing, Engineering & Mathematics, Western Sydney University, Sydney, Australia

ABSTRACT

A new iterative-analytical approach to determining the static behaviour of a cracked rotor has been developed and applied to a statically indeterminate model. The model subjects the cracked shaft to out-of-plane bending due to the inclusion of an offset dynamic force. The interaction between fixed supports and the variable shaft stiffness caused by a breathing crack make the model analytically unsolvable. The presented iterative algorithm for determining the breathing state of the crack makes the model analytically solvable for the support reactions and the elastic deflections. The algorithm rapidly converges, requiring typically fewer than 4 iterations to achieve stable results. The breathing response for a particular set of model parameters has been evaluated and is presented.

1. INTRODUCTION

Cracked shafts in rotating machinery can lead to catastrophic mechanical failure and costly loss of productivity. Early detection of surface cracks through vibration diagnostics is of great interest in heavy industry. Vibration characteristics of cracked rotors are still not completely understood. Numerical simulations play an important role in current research. Much of this research has been conducted into the problem of mathematically modelling the mechanical behaviour of a cracked rotor. Approaches to doing this have varied depending on the aim of the researcher. Static and quasi-static problems have been frequently studied using 3D finite element models that use nonlinear contact surfaces to simulate a crack (Bachschnid and Tanzi, 2004) (Rubio et al., 2014). Another technique used to statically model cracked rotors uses Euler beam theory and accounts for the crack by a discontinuity in the rotation of the shaft at the crack location the value of which is determined using the strain energy release rate (SERR) (Rubio et al., 2011).

For studying dynamic problems like critical speeds, and shaft orbital characteristics, it is common to model the shaft using beam finite elements with the crack's influence accounted for a reduced second moment of area for one or more of the elements (Spagnol and Wu, 2014) (Al-Shudeifat and Butcher, 2011).

The reduced section modulus at the crack location is a function of the opening percentage (i.e. the breathing state) of the crack. This in turn is related to the bending direction of the shaft at the crack location. The crack element will only assume the rigidity of an un-cracked shaft when the crack is fully closed.

Equations for the approximate 2nd moments of area were derived by Al-Shudeifat and Butcher (2011) for the case of a horizontal shaft subject only to static weight forces. These equations were developed further by Spagnol and Wu (2014) to consider dynamic forces in a Jeffcott rotor. This paper presents an iterative method of analysing the breathing of a statically indeterminate cracked rotor subject to out of plane bending loads.

2. MODEL DESCRIPTION

Consider a rotor supported by fixed ends is subjected to a distributed weight force, $m_s g/L$, two concentrated weight forces, $m_d g$, and dynamic force due to an unbalanced mass, F_{un} . A crack exists at $z = L_0$ which is modelled as region of the shaft of length L/n with a reduced stiffness, where n is an integer greater than 1 and L is the length of the shaft. The amount by which the stiffness is reduced depends on the crack's breathing state. The concentrated mass forces are from two discs mounted to the shaft, with the unbalance mass presenting in one of them. The rotation of the shaft is quantified by the angular displacement, θ , between midpoint of the crack face and the negative global Y axis (shown in Figure 1). The phase of the unbalanced mass is the angle β , from the crack front.

A method for determining the static behaviour of this model with a crack located between the two discs is as follows. Because the shaft is supported by cantilevers at both ends, the problem is statically indeterminate. Thus the support reactions are dependent on the shaft's stiffness. The shaft's stiffness is dependent on the breathing state of the crack.

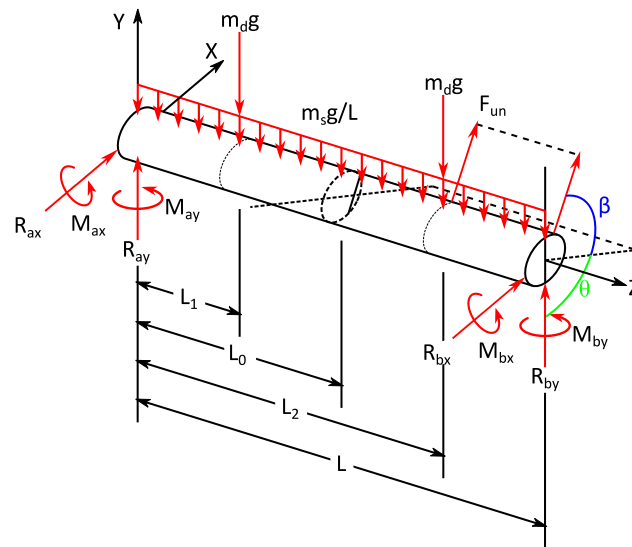


Figure 1: A 3 dimensional free body diagram of the shaft model. Note the crack presence at $z = L_0$.

The breathing state is dependent on the direction of the bending moment vector at the crack location relative to the shaft's rotation angle. Lastly the bending moment's magnitude and direction at the crack location is dependent on the magnitudes of the support reactions. This is essentially a closed circle of interdependence which cannot be analytically resolved.

2.1 Proposed method of solving the model

To solve this problem an iterative process will be used. The steps of this process are summarized below:

Step 1: Select an initial guess for the breathing state (or effective bending) angle, ϕ .

Step 2: Use the breathing function approximations to obtain the 2nd moments of area and product of area for the crack section about the global coordinate axes.

Step 3: Calculate the principle 2nd moments of area of the crack section; I_u and I_v . Calculate the angle between the principle axes and the global axes; α .

Step 4: Transform the weight forces and unbalance force from the global to principle coordinate systems.

Step 5: Using the 1st and 2nd Moment Area Theorems, solve for the support reactions in the planes of both principle axes. The reduced 2nd moments of area I_u and I_v are used in proximity to the crack.

Step 6: Evaluate the direction of the bending moment vector at the crack location, ψ .

Step 7: Determine a new value for the breathing state angle, ϕ .

Step 8: Repeat steps 2 to 7 until a stable value for ϕ is obtained.

2.1.1 Second moments and product of area for the crack region

The second moments of area for the cracked section are dependent on the shaft's rotation angle and the closed area of the crack. The closed area of the crack is a function of the shaft bending direction at the crack location. Approximations for the second moments of area and product of area about a rotating coordinate system, $y'-x'$ (whose Y axis is parallel to the bending direction vector, see Figure 2) derived by Al-Shudeifat and Butcher (2011) and Guo et al. (2013) are used. The first iteration of this process uses an arbitrary initial guess for the value of breathing state angle, ϕ .

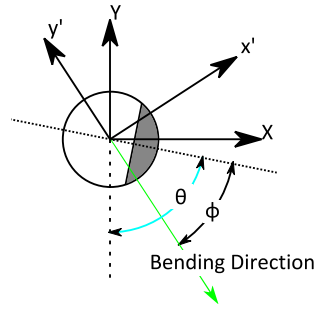


Figure 2: ϕ is the difference between the angle of the bending direction and the shaft rotation angle

2.1.2 Principle second moments of area for crack section

Using the second moments and product of area about the x' - y' axes, the second moment of area about the first principle axis is given by:

$$I_u = \frac{I_{x'} + I_{y'}}{2} + \sqrt{\left(\frac{I_{x'} - I_{y'}}{2}\right)^2 + I_{x'y'}^2} \tag{1}$$

And for the second principle axis:

$$I_v = \frac{I_{x'} + I_{y'}}{2} - \sqrt{\left(\frac{I_{x'} - I_{y'}}{2}\right)^2 + I_{x'y'}^2} \tag{2}$$

The angle of the principle axis with respect to the global coordinate system is given by:

$$\alpha^* = \frac{1}{2} \tan^{-1} \left(\frac{2I_{x'y'}}{I_{x'} - I_{y'}} \right) \tag{3}$$

$$\alpha = \begin{cases} \alpha^* + \theta - \varphi & I_{x'} > I_{y'}, I_{x'y'} < 0 \\ \theta - \varphi & I_{x'} > I_{y'}, I_{x'y'} = 0 \\ \pi - \alpha^* + \theta - \varphi & I_{x'} > I_{y'}, I_{x'y'} > 0 \\ \frac{\pi}{4} + \theta - \varphi & I_{x'} = I_{y'}, I_{x'y'} < 0 \\ \theta - \varphi & I_{x'} = I_{y'}, I_{x'y'} = 0 \\ \frac{3\pi}{4} + \theta - \varphi & I_{x'} = I_{y'}, I_{x'y'} > 0 \\ \frac{\pi}{2} - \alpha^* + \theta - \varphi & I_{x'} < I_{y'}, I_{x'y'} < 0 \\ \frac{\pi}{2} + \theta - \varphi & I_{x'} < I_{y'}, I_{x'y'} = 0 \\ \frac{\pi}{2} + \alpha^* + \theta - \varphi & I_{x'} < I_{y'}, I_{x'y'} > 0 \end{cases} \tag{4}$$

2.1.3 Force transformation into principle axes

The unbalance force requires that bending in two planes be considered. When the crack is not fully closed, its section will be irregular and the principle axes of the cross section will normally not be aligned with the global coordinate axes (see Figure 3).

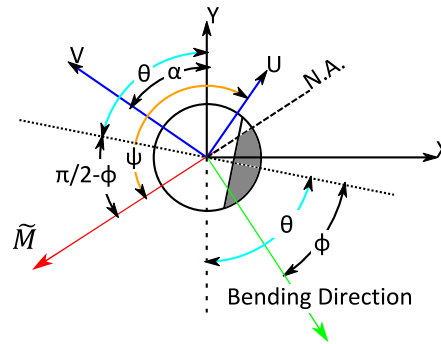


Figure 3: Relationship between bending moment, bending direction, coordinate axes and the effective angle ϕ

The angle α is defined as the angle between the second principle axis of the cracked section and the global positive Y axis. A positive value for α corresponds with principle axes that are rotated anticlockwise from the global coordinate axes. The load forces of the model need to be transformed into components that act in the direction of the principle axes.

The weight forces can be expressed in principle coordinates as

$$m_i g_u = m_i g \sin \alpha \tag{5}$$

$$m_i g_v = m_i g \cos \alpha \tag{6}$$

The unbalanced force will typically have components that act in both the Y and X axes of the global coordinate system. These can be transformed into the principle coordinate axes as follows

$$F_{unV} = F_{un} \sin \left(\theta + \beta - \alpha - \frac{\pi}{2} \right) \tag{7}$$

$$F_{unU} = F_{un} \cos \left(\theta + \beta - \alpha - \frac{\pi}{2} \right) \tag{8}$$

2.1.4 Shear forces and bending moments in the principle planes

The shear force and bending moment diagrams for each of the principle axes can be now drawn. As the support reactions are still unknown they will be represented by pronumerals. The analysis will now consider bending in the plane of second principle axis (V-axis). The same methodology is applied to bending in the plane of the first principle axis (U-axis). The shear force diagram (SFD) for the V-Z plane is shown below.

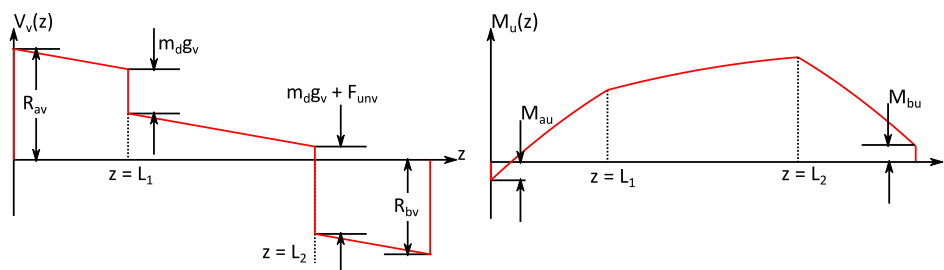


Figure 4: Shear force (left) and bending moment (right) diagrams in the plane in of the second principle axis

The bending moment diagram (BMD) for the V-Z plane is obtained by integration of the SFD. The curve of the bending moment diagram is discontinuous due to the influence from the concentrated weight forces and the unbalanced force. Support reaction moments M_{au} and M_{bu} are not yet known.

The bending moment curve shown in Figure 4 has an equation of the form

$$M_u(z) = -1 \times \begin{cases} \frac{m_s g_v}{2L} z^2 + R_{av} z + M_{au} & 0 < z \leq L_1 \\ \frac{m_s g_v}{2L} z^2 + m_d g_v (z - L_1) + R_{av} z + M_{au} & L_1 < z \leq L_2 \\ \frac{m_s g_v}{2L} z^2 + m_d g_v (2z - L_1 - L_2) + F_{unv} (z - L_2) + R_{av} z + M_{au} & L_2 < z \leq L \end{cases} \quad (9)$$

Note that the equation for the bending moment in the U-Z plane does not have the multiplicative factor of -1 used in equation 9.

2.1.5 Solving for the support reactions

By treating the shaft as an Euler beam, the moment area theorem can be applied to solve for the support reactions. The influence of the crack is accounted for by the reduced second moment of area when integrating the bending moment.

The fixed ends of the shaft mean that displacement and rotation of the shaft at the supports will be zero. The resulting moment area equations will be:

$$\int_0^L \frac{M(z)}{EI} dz = 0 \quad (10)$$

$$\int_0^L z \frac{M_u(z)}{EI} dz = 0 \quad (11)$$

Evaluating both of these integrals yields a system of two simultaneous equations which are solvable for the support reactions using Cramer's rule.

$$R_{av} = \frac{(-m_s g_v b_{1s} - m_d g_v b_{1d} - F_{unv} b_{1f}) a_{22} - (-m_d g_v b_{2d} - F_{unv} b_{2f} - m_s g_v b_{2s}) a_{12}}{a_{11} a_{22} - a_{21} a_{12}} \quad (12)$$

$$M_{au} = \frac{a_{11} (-m_d g_v b_{2d} - F_{unv} b_{2f} - m_s g_v b_{2s}) - a_{21} (-m_s g_v b_{1s} - m_d g_v b_{1d} - F_{unv} b_{1f})}{a_{11} a_{22} - a_{21} a_{12}} \quad (13)$$

In equations 12 and 13 a_{ij} and b_{ij} are functions of model geometry and crack breathing state. Their values for cases where the crack is located between the two discs are shown below.

$$a_{11} = \frac{1}{EI} \left(\frac{L^2}{2} - \frac{LL_0}{n} \right) + \frac{1}{EI_u} \left(\frac{LL_0}{n} \right) \quad (14)$$

$$a_{12} = \frac{1}{EI} \left(L - \frac{L}{n} \right) + \frac{1}{EI_u} \left(\frac{L}{n} \right) \quad (15)$$

$$a_{21} = \frac{1}{EI} \left(\frac{L^3}{3} - \frac{L^3}{12n^3} - \frac{LL_0^2}{n} \right) + \frac{1}{EI_u} \left(\frac{L^3}{12n^3} + \frac{LL_0^2}{n} \right) \quad (16)$$

$$a_{22} = \frac{1}{EI} \left(\frac{L^2}{2} - \frac{LL_0}{n} \right) + \frac{1}{EI_u} \left(\frac{LL_0}{n} \right) \quad (17)$$

$$b_{1s} = \frac{1}{EI} \left(\frac{L^2}{6} - \frac{L^2}{24n^3} - \frac{L_0^2}{2n} \right) + \frac{1}{EI_u} \left(\frac{L^2}{24n^3} + \frac{L_0^2}{2n} \right) \quad (18)$$

$$b_{1d} = \frac{1}{EI} \left(L^2 + \frac{L_1^2}{2} + \frac{L_2^2}{2} - LL_1 - LL_2 - \frac{LL_0}{n} + \frac{LL_1}{n} \right) + \frac{1}{EI_u} \left(\frac{LL_0}{n} - \frac{LL_1}{n} \right) \quad (19)$$

$$b_{1f} = \frac{1}{EI} \left(\frac{L^2}{2} - LL_2 + \frac{L_2^2}{2} \right) \quad (20)$$

$$b_{2s} = \frac{1}{EI} \left(\frac{L^3}{8} - \frac{L_0^3}{2n} - \frac{L^2 L_0}{8n^3} \right) + \frac{1}{EI_u} \left(\frac{L_0^3}{2n} + \frac{L^2 L_0}{8n^3} \right) \quad (21)$$

$$b_{2d} = \frac{1}{EI} \left(\frac{2L^3}{3} - \frac{L^2 L_2}{2} - \frac{L^2 L_1}{2} + \frac{L_1^3}{6} + \frac{L_2^3}{6} - \frac{L^3}{12n^3} - \frac{LL_0^2}{n} + \frac{LL_0 L_1}{n} \right) + \frac{1}{EI_u} \left(\frac{L^3}{12n^3} + \frac{LL_0^2}{n} - \frac{LL_0 L_1}{n} \right) \quad (22)$$

$$b_{2f} = \frac{1}{EI} \left(\frac{L^3}{3} - \frac{L^2 L_2}{2} + \frac{L_2^3}{6} \right) \quad (23)$$

The support reactions in the plane of the first principle axis can be calculated by substituting the 2nd moment of area and transformed loads for that plane into equations 12 – 23.

2.1.6 Evaluating the bending moment at the crack location

The components of the bending moment at the crack location in principle coordinates are given below. Note the difference in the signs of the terms, which is simply a property of the coordinate system chosen.

$$M_u(L_0) = -\frac{m_s g_v}{2L} L_0^2 - (R_{av} + m_d g_v) L_0 - M_{au} + m_d g_v L_1 \quad (24)$$

$$M_v(L_0) = \frac{m_s g_u}{2L} L_0^2 + (R_{au} + m_d g_u) L_0 + M_{av} - m_d g_u L_1 \quad (25)$$

With the bending moments about both principle axes known, the direction of the bending moment needs to be evaluated. An angle ψ is defined at the angle between the bending moment vector and the positive direction of the first principle axis (U-axis). The range of ψ is restricted to $0 < \psi < 2\pi$ with anticlockwise rotation being positive. It is evaluated below

$$\psi^* = \tan^{-1} \left(\left| \frac{M_v(L_0)}{M_u(L_0)} \right| \right) \quad (26)$$

$$\psi = \begin{cases} \psi^* & M_u(L_0) > 0 \quad M_v(L_0) \geq 0 \\ 2\pi - \psi^* & M_u(L_0) > 0 \quad M_v(L_0) < 0 \\ \pi - \psi^* & M_u(L_0) < 0 \quad M_v(L_0) \geq 0 \\ \pi + \psi^* & M_u(L_0) < 0 \quad M_v(L_0) < 0 \end{cases} \quad (27)$$

2.1.7 Effective bending angle

In this model it is assumed that the neutral axis of the crack section is parallel to the bending moment vector. The crack's breathing state is a function of orientation of the neutral plane, the bending direction and the shaft's rotation angle. At this point it is worth considering the relationship between these vectors with the aid of a diagram of the crack section. Both the global and principle coordinate axes are shown in the diagram below.

From Figure 3, it is apparent that ϕ is a function of the shaft rotation angle θ , the angle between the principle axes and the global axes α , and the angle between the bending moment vector and the first principle axis ψ .

$$\phi = \pi + \theta - \alpha - \psi \quad (28)$$

Equation 28 will give an estimate for the value of ϕ that will be more accurate than either the initial guessed value or the value obtained from any subsequent iterations. Each repetition of the process, described above, will yield a more accurate value for ϕ . Because of the interdependence between ϕ , the shaft stiffness, bending moments and deflection, the accuracy of these variables is also improved. For practical purposes, convergence is typically achieved within 4 iterations regardless of the initial guess value for ϕ .

3. RESULTS FOR BREATHING RESPONSE

The breathing response of the model has been evaluated for a set of model parameters that are outlined in Table 1. The breathing state can be completely described by effective bending angle ϕ and qualitatively understood by the crack opening state. Both variables have been evaluated and are presented.

Table 1: List of parameters used to evaluated the breathing response

Parameter	Value	Parameter	Value
Shaft length, L (m)	0.725	Disc 2 location, L_2 (m)	0.543
Shaft radius, R (m)	0.00635	Reduce section proportion, n	100
Shaft Young's modulus, E (GPa)	210	Relative crack location, λ	Varied
Shaft density, ρ (kg/m ³)	7800	Relative crack depth, μ	0.75
Disc mass (both discs), m_d (kg)	0.5	Unbalance force ratio, η	10
Disc 1 location, L_1 (m)	0.181	Unbalance force phase, β (°)	90

The evaluation of the breathing response is performed using the following parameter definitions for mass unbalance force, F_{un} , crack depth, h and crack location, L_0 :

$$\eta = \frac{m_s g + 2m_d g}{F_{un}} \tag{29}$$

$$\mu = \frac{h}{R} = \frac{2h}{D} \tag{30}$$

$$\lambda = \frac{L_0}{L} \tag{31}$$

The effective breathing angle for several shaft rotation angles has been evaluated for every possible crack location (i.e. from $\lambda=0$ to $\lambda=1$) using the presented algorithm. The results are presented in Figure 5. Note that terms ϕ_1 , ϕ_2 , ϕ_3 & ϕ_4 shown in Figure 5 are the effective bending angles at which the crack starts to close, becomes fully closed, starts to reopen and is fully open again respectively. Their values are dependent on the crack depth and are calculated using equations derived by Al-Shudeifat and Butcher (2011).

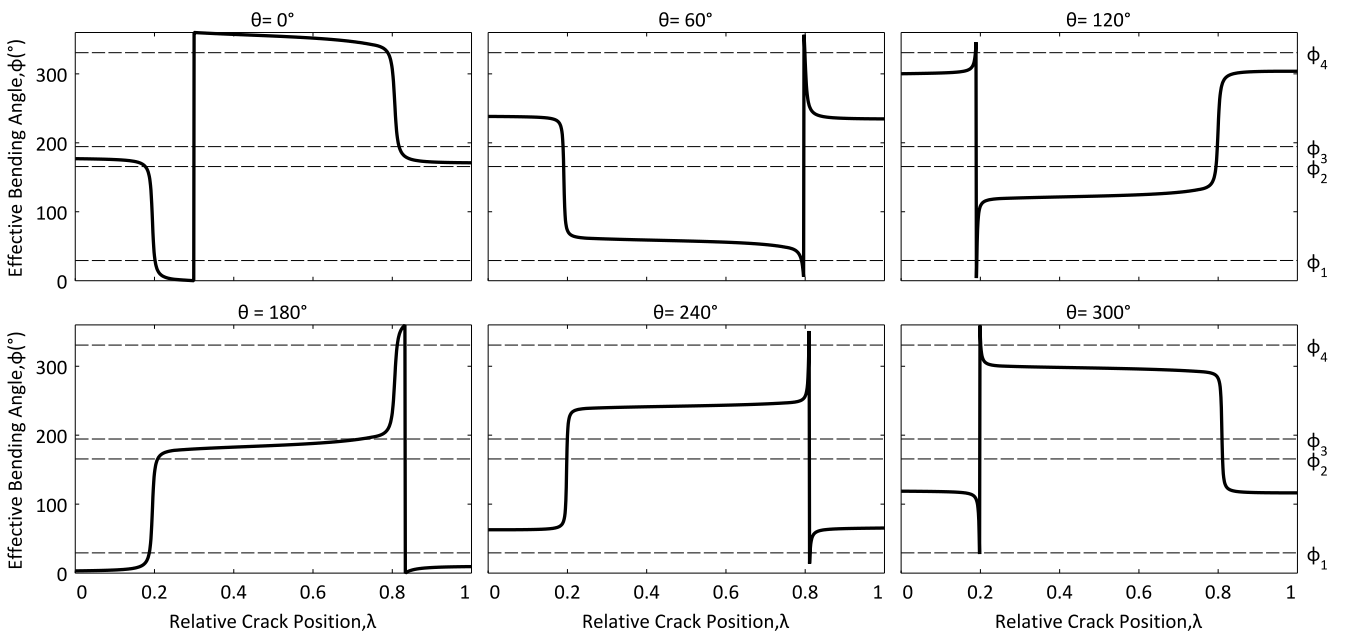


Figure 5: Effective bending angle throughout the shaft length for rotation angles of 0°, 60° and 120°. Model parameters are: $\beta=90^\circ$, $\mu=0.75$ and $\eta=10$

The apparent discontinuities in Figure 5 near $\lambda=0.2$ and $\lambda=0.8$ are simply the result restricting the numerical value of ϕ to $0 < \phi < 2\pi$. The results are mostly intuitive in so far as the bending direction at the supports is close to 180° out of phase with the bending at the mid span. The crack opening state throughout the shaft rotation has been qualitatively evaluated for 6 crack location scenarios. Three crack opening states are considered, fully open, partially open and fully closed. The results are presented in Figure 6.

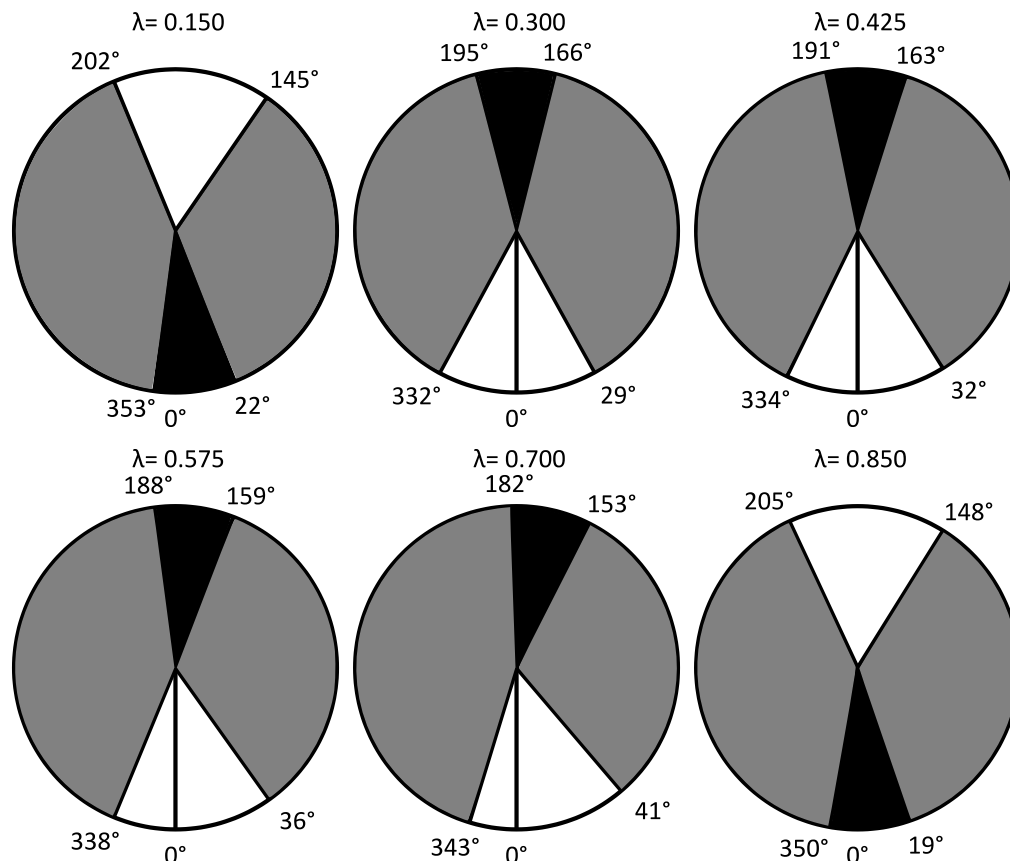


Figure 6: Crack opening states throughout the shaft rotation. White regions of the pie charts are where the crack is fully open, grey for partially open and black for fully closed. Model parameters are: $\beta=90^\circ$, $\mu=0.75$ and $\eta=10$

The crack opening states shown in Figure 6 are consistent with the effective bending angles in Figure 5 and exhibit the same intuitive outcome of oppositely signed curvature near the ends of the shaft ($\lambda=0.15$ and $\lambda=0.85$) when compared to the mid span ($\lambda=0.3$, $\lambda=0.425$, $\lambda=0.575$ and $\lambda=0.7$). It is also worth noting the asymmetry of the open and closed regions of the rotation. This is the result of the unbalanced mass whose phase leads the crack by 90° .

4. CONCLUSIONS

A new method is proposed for solving statically and analytically indeterminate cracked rotor subject to combined weight and dynamic loading has been developed by means of an iterative application of Euler beam theory. By determining the bending direction of the shaft at the crack location, the reaction forces and elastic deflections become analytically solvable. The crack opening state and effective bending angle for a particular set of model parameters has been evaluated. The results are similar those one might expect for balanced shaft. The slight deviation is expected due to the small though not trivial mass unbalance. The influence of the mass unbalance is more apparent when considering crack opening state throughout shaft rotation where a noticeable asymmetry arises thanks to the phase offset of the unbalanced mass. The proposed method has potential to be adapted for use in quasi-static and beam finite element studies of similar cracked rotor models.

ACKNOWLEDGEMENTS

The authors wish to thank Dr Keqin Xiao for his continued guidance and insight throughout this research.

REFERENCES

- AL-SHUDEIFAT, M. A. & BUTCHER, E. A. 2011. New breathing functions for the transverse breathing crack of the cracked rotor system: Approach for critical and subcritical harmonic analysis. *Journal of Sound and Vibration*, 330, 526-544.
- BACHSCHMID, N. & TANZI, E. 2004. Deflections and strains in cracked shafts due to rotating loads: a numerical and experimental analysis. *International Journal of Rotating Machinery*, 10, 283-291.
- GUO, C., AL-SHUDEIFAT, M., YAN, J., BERGMAN, L., MCFARLAND, D. & BUTCHER, E. 2013. Application of empirical mode decomposition to a Jeffcott rotor with a breathing crack. *Journal of Sound and Vibration*, 332, 3881-3892.
- RUBIO, L., MUÑOZ-ABELLA, B. & LOAIZA, G. 2011. Static behaviour of a shaft with an elliptical crack. *Mechanical Systems and Signal Processing*, 25, 1674-1686.
- RUBIO, L., MUÑOZ-ABELLA, B., RUBIO, P. & MONTERO, L. 2014. Quasi-static numerical study of the breathing mechanism of an elliptical crack in an unbalanced rotating shaft. *Latin American Journal of Solids & Structures*, 11, 2333-2350.
- SPAGNOL, J. P. & WU, H. Breathing mechanism of a cracked rotor subject to non-trivial mass unbalance. INTER-NOISE and NOISE-CON Congress and Conference Proceedings, 2014. Institute of Noise Control Engineering, 6404-6410.